NJC

Accepted Manuscript

This article can be cited before page numbers have been issued, to do this please use: J. Gazowska, H. Czapor-Irzabek, E. Chmielewska, P. Kafarski and T. Janek, *New J. Chem.*, 2018, DOI: 10.1039/C8NJ01158C.

View Article Online
DOI: 10.1039/C8NJ01158C

NJC

ARTICLE

Aminobisphosphonates based on cyclohexane backbone as coordinating agents for metal ions. Thermodynamic, spectroscopic and biological studies.

Received 00th January 20xx,
Accepted 00th January 20xx

DOI: 10.1039/x0xx00000x

www.rsc.org/

J. Gałęzowska,*[a] H. Czapor-Irzabek,[b] E. Chmielewska,[c] P. Kafarski[c] and T. Janek[a]

Single- and double-amino-bisphosphonates were synthesized and tested for coordination capabilities towards Ca^{2+}, Mg^{2+}, Cu^{2+} and Ni^{2+} metal ions by means of potentiometry, UV-vis spectroscopy, mass spectrometry (ESI-MS) and isothermal titration calorimetry (ITC), as well as for cytotoxic activity by MTT [(3-(4,5-dimethylthiazol-2-yl)-2,5-diphenyltetrazolium bromide] assay. Half minimal inhibitory concentrations (IC_{50}) were determined with respect to two cell lines (human melanoma A375 and human colorectal adenocarcinoma HT29). Bearing the structure of compounds on cyclohexane ring allowed for a slight reduction of high hydrophilic character of studied bisphosphonates (BPs). The ligands efficiently bind examined metal ions forming complex equilibria with diversified stoichiometry of equimolar, polynuclear species and biscomplexes. Both ligands as well as their Ca^{2+} and Mg^{2+} complexes show selective antiproliferative activity toward studied cancer cell lines. Given thermodynamic and biological data, it can be assumed that ligands are good candidates for linking compounds that may be used in the design of new drug delivery systems. In such approach one bisphosphonate moiety acts as a bone-targeting molecule, while another molecule can be readily attached to the second donor function (primary amine or bisphosphonate).

Introduction

Bisphosphonates (BPs) are a group of compounds with two phosphonate functions attached to a geminal carbon atom that has found various medical applications.[1–8] Thanks to such features like; 1) structural similarity of phosphonic group to phosphate, 2) low biodegradability,[9] 3) possibility to accommodate metal ions with various ionic radii[10–12] and 4) presence of P-C-P backbone, that provides bone delivery properties followed by antiresorptive effects,[213] BPs have become particularly important drugs in bone-related diseases. They are first choice drugs for osteoporosis,[14] act as therapeutic drug carriers,[15] imaging bone-targeting tools[16] and bone-pain palliation relievers.[17–19] However, in every aspect of use; BPs reveal side effects among which osteonecrosis of the jaw (95% of patients treated with the most potent heterocyclic N-BPs),[20,21] atrial fibrillation,[22] hypocalcemia, over-suppression of bone turnover and other complications[23] can be listed. These side-effects along with low bioavailability of BP are the reason why there is still a need to design new ligands with better characteristics. However, nowadays research goals are rather aimed at design of locally administrated drugs, materials and conjugated delivery tools[24–29] than designing new bisphosphonates of subsequent generations,[30] although such BPs are also desired especially with lower binding affinity which produce e.g. more rapid decrease in fracture risk.[31]

At the same time clinical findings suggest that some of BPs reduce the burden of bone cancer and increase the survival rate among patients. Most probably BP have a direct effect on some types of cancer cells and reveal antitumor effect.[32–34]

We have synthesized three, based on a cyclohexane skeleton, aminobisphosphonic acids (amino-BP) which chemical structures are depicted in Fig. 1. L^1 contain one (single-amino-BP) and L^2, L^3 two bisphosphonic moieties (double-amino-BP). Ligands were shown previously in our patent.[35] L^3 was also prepared almost in parallel by Goldeman et al.,[36] however using a different synthetic approach. For all studied ligands we used three-component reaction of cyclic diamines with triethyl orthoformate and diethyl phosphite. It is perhaps the most general and common procedure

[a] Department of Inorganic Chemistry, Wrocław Medical University, Borowska 211A, 50-556 Wrocław, Poland. E-mail: joanna.galezowska@umed.wroc.pl
[b] Laboratory of Elemental Analysis and Structural Research, Wrocław Medical University, Borowska 211A, 50-556 Wrocław, Poland
[c] Department of Bioorganic Chemistry, Faculty of Chemistry, Wrocław University of Science and Technology, Wybrzeże Wyspianskiego 27, 50-370, Wrocław, Poland

Electronic Supplementary Information (ESI) available: **Fig. S1** Comparison of protonation constants single and double di- and bisphosphonic acids, literature data. **Fig S2.** UV-vis spectra for Cu^{2+} complexes in a broad pH range (measured and calculated). **Fig. S3**. UV-vis spectra for Ni^{2+} complexes in a broad pH range (measured and calculated). **Tab. S1**. Stability constants ($\log\beta$) of Cu^{2+} and Ni^{2+} complexes with L^1 and L^2 obtained by UV-vis titrations. **Fig. S4**. ESI-MS data for ligands alone. **Tab. S2.** ESI-MS data for $L^{1,2,3}/Cu^{2+}$, Ni^{2+}, Ca^{2+} and Mg^{2+} complexes. **Figure S5.** ESI-MS data for $M^{2+}/L^{1,2,3}$ complexes. **Fig. S6**. Species distribution of studied systems with Ca^{2+} and Mg^{2+} calculated from equilibrium constants using IC_{50} concentrations conditions. **Tab. S3**. Experimentally measured molar extinction coefficients (ε) and absorbance maxima (λmax) for ligands which concentration was determined by UV-vis. **Fig. S7.** Standard deviation around ITC fit for studied systems. **Fig. S8**. Effects of bisphosphonates and Mg^{2+} or Ca^{2+} bisphosphonates complexes on the viability of melanoma A375 cells (A-D) and HT29 cells (E-H). **Fig. S9 (several)**. NMR and mass spectrometry ligands alone - synthetic details. See DOI: 10.1039/x0xx00000x.

View Article Online
DOI: 10.1039/C8NJ01158C

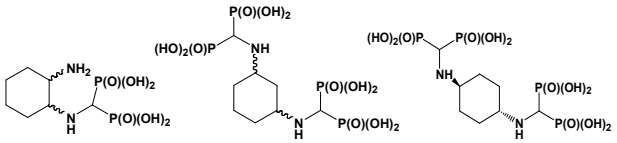

Fig. 1. Chemical structures of studied ligands

to synthesize N-substituted aminomethylenebisphosphonic acids.[37–39] Since this reaction usually gives the mixtures of products, that are difficult to separate, the crude esters are commonly hydrolyzed with concentrated hydrochloric acid and the desired bisphosphonic acids are isolated in moderate to good yields. Introducing cyclohexane as a backbone for the ligands had three purposes: 1) to reduce the hydrophilicity of phosphonic groups, 2) to provide a steric barrier that prevents the coordination of metal ion by more than one functional group and 3) to allow to exhibit cytotoxic activity, since it has been proven that aromatic BPs reveal significantly higher activity than aliphatic ones.[36] Antiproliferative activity of L^3 has been previously studied with respect to MCF-7 human breast cancer cells, J774E mouse macrophages and HL-60 human promyelocytic leukemia cells lines, revealing differentiated, mild activity.[36] The aim of this work was to study the physico-chemistry of interactions between synthesized ligands and various metal ions. We focused on metal ions of biological importance: Ca^{2+}, Mg^{2+} but because of the wide binding capacity of BPs, examined coordination properties of L^{1-3} towards chosen transition metals as well. We have chosen Cu^{2+} and Ni^{2+} ions due to their relatively well-described spectral response to amino-BPs binding.

The interactions with Ca^{2+} ions are important in particular because of the binding of BPs to hydroxyapatite. This binding opens up a cascade of chemical and biological events that lead to antiresorptive action of BPs in general. It has been found that the formation of Ca^{2+}/BP complexes is either the first event before drug introduction into the bone structure[40,41] or a competitive reaction to bone surface absorption,[41] therefore this binding and its physico-chemistry has to be taken into account.

An important factor of pharmacological activity of BPs is their chemical nature/state in blood plasma (free acid, complex, charge, polarity, etc.). Because the concentration of Ca^{2+} in blood plasma at pH 7.4 is maintained at ~ 3mM and of Mg^{2+} at ~ 1mM,[42] it is highly likely that the majority of introduced BP is bound to Ca^{2+}, Mg^{2+} and other species e.g. Na^+. Therefore, quantitative thermodynamic studies and biological tests were performed for calcium and magnesium cations with the studied ligands. An attempt was also made to predict the dominant species found in the solution under the conditions of biological studies in order to indicate active species.

An additional goal, considering literature examples of antitumor effects revealed by BPs in general, as well as antiproliferative characteristics of L^3, was to test anti-cancer activity of both; free ligands and their Ca^{2+} and Mg^{2+} complexes in respect to cell lines of colon adenoma and melanoma skin cancer, the most common malignant tumors worldwide. The results were compared experimentally to incadronate (*N*-(cycloheptyl)-aminomethylenebisphosphonic acid), a commercially available BP that chemical structure is the closest to the structure of studied ligands.

Results and Discussion

Acid-base properties of ligands

L^1 as a fully protonated ligand possess six dissociable protons (H_6L); four belong to phosphonic functions, one to primary amine and one to tertiary amine NH^+R. Under applied conditions four of protonation constants could be determined via potentiometry and the results are given in Table 1. All estimated values can be attributed to deprotonation of phosphonic groups. This assumption agrees with literature data for similar ligands; p*K*s of 1-hydroxy-4-aminopropilydenediphosphonic acid are as follows: 10.95_{amine}, $9.80_{phosphonate}$, $6.01_{phosphonate}$, $2.56_{phosphonate}$,[43] pamidronic acid (3-amino-1-hydroxypropylidene-1,1-bisphosphonate): 13.06_{amine}, $10.30_{phosphonate}$, $5.85_{phosphonate}$, $1.80_{phosphonate}$, $<1.20_{phosphonate}$.[42] For a ligand with an analogous structure, however with no NH^+R amine; N-cycloheptyl-alkylaminomethane-1,1-diphosphonic acid, measured p*K* values are: 8.72, 4.76 and 2.07,[44] and all belong to deprotonation procesess of phosphonic moieties. For L^1 examined here, it was possible to approximate the highest p*K* value and it was calculated as 12.59(8). This value most probably can be assign to the NH_3^+ group. However, because the measurements were carried out only up to pH 12 this value is unreliable and was excluded from the calculations. The last, basic proton of L^1 dissociates above pH 13[45] from the nitrogen atom of NHR^+ function. This deprotonation constant could not be estimated under pH titrations as well. In this case, we use the neglect approach in the calculation of the dissociation of NH^+R group, as suggested by Kurzak et al.[45] and Szpak et al.[44] for similar ligands, where it is not possible to obtain reliable p*K* constants p*K*>13. So high p*K* value of NH^+R (as well as NH_3^+) was observed in similar compounds and was explained by the existence of intramolecular N-H···$O_{phosphonate}$ hydrogen bond.[44] It was proven that such a H-bond stabilizes the structure of monosubstituted piperid-1-ylmethane-1,1-diphosphonic acids in solid state and is a reason to create stabile *head to head* dimers by molecules of free ligands.[46] In case of L^1 the possibilities to form H-bonds are two: eighter using N(1) or N(2), both would lead to increase the p*K*s of nitrogen-containg groups, what most likely takes place. Probable zwitterionic structure of L^1 is depicted on Fig. 2. The lowest deprotonation step which occurs on phosphonic moiety (pH <<2) could not be detected, what is very common for BPs.

Fully protonated L^2 and L^3 ligands behave like $H_{10}L$ acids. Groups capable of deprotonating are the following: two NH^+R functions that release two protons and two bisphosphonic moieties releasing a total of eight protons. However, only four protonation

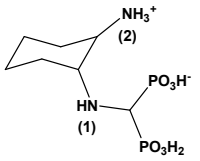

Fig. 2. Zwitterionic form of L^1.

DOI: 10.1039/C8NJ01158C

Table 1. Protonation constants of studied ligands at 25°C and *I*=0.1M (KCl). All estimated values belong to phosphonic moietes. Due to very basic constants of amine functions, which do not deprotonate in measurable range ligands, correct notifications for studied ligands, following literature[44] should be: L^1=HL, L^2,L^3=H_2L, however here it was omitted for simplicity.

Species	L^1		L^2		L^3	
	log*β*	log*K*	log*β*	p*K*	log*β*	p*K*
HL	9.76(7)	9.76	9.80(3)	9.80	9.54(3)	9.54
H_2L	16.41(5)	6.65	18.20(3)	8.40	17.92(3)	8.38
H_3L	20.03(5)	3.62	24.89(5)	6.69	24.13(6)	6.21
H_4L	21.58(5)	1.55	29.89(5)	5.00	28.88(5)	4.75
H_5L	-	-	31.41(7)	1.52	-	-

constants for L^3 and five for L^2 could be calculated and are given in Table 1. All estimated values belong to phosphonic functions. Both; the lowest (<pH 1) and the most basic (>pH 12) protonation constants, as in case of L^1, could not be determined due to the limitations of the method. Studies of double BPs (tetraphosphonic acids) in terms of their acid-base properties are rare,[49,50] what excludes any straightforward comparison to analogues studied in literature. A comparison to a different group of multiphosphonates: *N*-methylenephosphonic acids,[51–53] which have gained more scientific attention, is not possible due to the well-known fact of significant changes in acid-base diphosphonate properties when combined with a geminal carbon atom in comparison with ligands possessing two phosphonic functions, but differently connected (see Fig. S1, SI). We assume that two very basic p*K*s for NH^+R groups were not determined under the conditions of experiment, for the same reason as for L^1, because they lie above pH 13 due to hydrogen bond formation involving a nitrogen atom from NH^+R as a donor and oxygen from the phosphonic function as an acceptor.

ESI-MS spectra of all studied ligands showed their high tendency to create polimeric structures (Fig. S4, SI), that confirms the possibility of formation of internal hydrogen bonds providing stabilisation of aggregates in solution (Fig. S4, SI).

Table 2. Stability constants (log*β*) of M^{2+} complexes with L^1 obtained by potentiometry at 25°C and *I*=0.1M (KCl).

Species	L^1			
M:H:L	Ca^{2+}	Mg^{2+}	Cu^{2+}	Ni^{2+}
log*β*[MH_2L]	19.89(4)	-	-	-
log*β*[MHL]	13.68(6)	13.19(3)	17.71(3)	14.56(9)
log*β*[ML]	**4.86(14)**	**5.08(4)**	**11.73(4)**	**10.30(2)**
log*β*[$MH_{-1}L$]	-5.41(7)	-	-	-
log*β*[MH_2L_2]	-	-	-	
log*β*[MHL_2]	18.33(13)	17.57(14)	-	23.19(10)
log*β*[ML_2]	8.93(9)	8.78(8)	16.69(6)	16.65(8)
log*β*[$MH_{-1}L_2$]	-	-2.32(5)	6.69(6)	8.04(9)
log*β*[$MH_{-2}L_2$]	-	-	-3.52(5)	-2.52(10)
log*β*[M_2L]	-	-	18.78(5)	-
pK_a[MH_2L]	6.21	-	-	-
pK_a[MHL]	8.33	8.11	5.98	4.26
pK_a[ML]	10.27	-	-	-
pK_a[$MH_{-1}L$]	-	-	-	-
pK_a[MH_2L_2]	-	-	-	-
pK_a[MHL_2]	9.40	8.79	-	6.54
pK_a[ML_2]	-	11.10	10.00	8.61
pK_a[$MH_{-1}L_2$]	-	-	10.21	10.56
pK_a[$MH_{-2}L_2$]	-	-	-	-

Numbers in parentheses denote statistical errors on the last significant digits.
Existence of hydroxocomplexes[47,48] was considered in all calculations (M^{2+}/L^{1-3}).
Charges were omitted for clarity.

Metal Complexes

Up to date numerous papers have been devoted to coordination properties of BPs towards Ca^{2+}/Mg^{2+}[42–44,54–57] (alkaline earth metal ions) and Cu^{2+},[42,45,58–60] significantly less to Ni^{2+}[61–63] (transition metal ions). Only very few data can be found for complexation of ligands, that contain more than one bisphosphonic functions, toward any kind of metal ion.[50] The available data indicate, as expected, taking into account different chemical properties of these metal ions, that the equilibrium in the solution varies significantly with alkaline earth metals and transition metal ions. However, certainly a common feature of BPs regardless of the metal ion is eagerness to create apart from monomeric complexes also oligonuclear species which were found both in solution[12] and solid state.[11] Such abilities lead to creation of complex equilibria of co-existence of monomeric and oligomeric species in a broad pH range,[12] what is expected for studied ligands as well. Towards this end we have used, apart from potentiometry, mass spectrometry (ESI-MS) in order to detect various stoichiometries of complexes, which calculations based on potentiometric titrations cannot distinguish. All peak assignments for ESI-MS were confirmed by comparison of calculated and experimental isotope distribution patterns.

It is also known, that the phenomenon of precipitation often accompany BP-complexation studies. Especially upon coordination of Ca^{2+} cations, precipitations were observed in wide pH ranges for several BPs,[42] however, precipitate might also occur in solution due to the interactions between phosphonic moieties that lead two or more ligand molecules to aggregation.[11,54,55] Herein such precipitations were also observed, details are given in Experimental Section, and these measurements were excluded from calculations.

Complexation of $Ca^{2+}$and Mg^{2+} . The complex formation equilibria in L^1/Ca^{2+} and L^1/ Mg^{2+} systems are similar to each other (Table 2, Fig. 3). Calculations based on potentiometric titrations revealed the existence of equimolar species and biscomplexes that occur in differently protonated forms in both systems. ML and ML_2 species coexist in the solution above pH 7. p*K* values of following deprotonations processes; $MH_2L \leftrightarrow MHL + H$, $MHL \leftrightarrow ML + H$ vary between 6.21 and 9.40 and for $MHL_2 \leftrightarrow ML_2 + H$ between 8.79 and 9.40 (Table 2). These values can be attributed to a stepwise deprotonation and coordination of oxygen atoms from phosphonic groups. In basic pH both ML and ML_2 type of species undergo hydrolysis to $MH_{-1}L$, $MH_{-1}L_2$ and $MH_{-2}L_2$ complexes which better can be described as; M(OH)L, $M(OH)L_2$ and $M(OH)_2L_2$, respectively. Since the p*K* values of reactions fall in a range of 10.27-11.1, they can be attributed to a deprotonation of water molecules, that is a common behaviour of amino-BPs complexes in high pH.[44] The presence of both; equimolar and biscomplexes, was confirmed by ESI-MS for Mg^{2+} (Table S2, Fig. S5, SI). For the Ca^{2+}/L^1 system, ML_3 complex was additionally detected by ESI-MS. In literature similar amino-BPs were confirmed to create ML_2 species in solution,[44,56,57] although the repulsion of highly negatively charged phosphonic groups makes such species rather unfavourable in general. Most likely due to this reason ML_3 complexes were not detected potentiometrically. No occurrence of polymeric complexes was detected.

Comparison of the stability constants of fully deprotonated ML species indicates that L^1 forms complexes with stability that is consistent with the literature data ($\log\beta_{CaL}$=4.86, $\log\beta_{MgL}$=5.08),[44,55–57] which also state that BP-Mg^{2+} complexes are slightly more stable than those of Ca^{2+} in general. However, it must be borne in mind that for BP type of compounds a simple

View Article Online
DOI: 10.1039/C8NJ01158C

Table 3. Stability constants (logβ) of M^{2+} complexes with L^2 and L^3 obtained by potentiometry at 25°C and I=0.1M (KCl).

Species	L^2				L^3			
M:H:L	Ca^{2+}	Mg^{2+}	Cu^{2+}	Ni^{2+}	Ca^{2+}	Mg^{2+}	Cu^{2+}	Ni^{2+}
logβ[MH_2L]	-	-	24.69(3)	24.43(3)	21.78(5)	21.62(10)	-	-
logβ[MHL]	16.05(4)	14.40(3)	18.89(3)	17.99(5)	13.72(6)	13.77(12)	18.09(9)	16.54(13)
logβ[ML]	**4.60(6)**	**4.66(4)**	**10.74(4)**	**8.77(6)**	**4.83(6)**	**4.95(10)**	**10.20(6)**	**8.33(8)**
logβ[$MH_{-1}L$]	-	-6.11(4)	-	-1.37(6)	-5.21(6)	-4.98(10)	-	-
logβ[MHL_2]	-	-	-	-	-	-	-	-
logβ[ML_2]	-	-	14.87(4)	12.79(10)	-	-	14.52(8)	-
logβ[$MH_{-1}L_2$]	-	-	3.96(4)	-	-	-	5.01(8)	0.88(15)
logβ[$MH_{-2}L_2$]	-	-	-	-8.67(9)	-	-	-4.53(7)	-9.52(9)
logβ[$M_2H_7L_2$]	-	-	65.89(17)	-	-	-	65.81(14)	-
logβ[$M_2H_6L_2$]	-	-	62.78(3)	-	-	-	62.42(8)	-
logβ[$M_2H_5L_2$]	55.81(6)	53.88(8)	57.86(10)	55.91(16)	-	-	-	-
logβ[$M_2H_4L_2$]	50.91(5)	48.11(5)	-	-	-	-	53.00(9)	-
logβ[$M_2H_3L_2$]	43.46(11)	40.19(10)	-	46.20(11)	-	-	47.27(10)	45.11(7)
logβ[M_2HL_3]	-	-	-	-	26.41(20)	-	-	-
pK[MH_2L]	-	-	-	-	-	-	-	-
pK[MHL]	-	-	5.80	6.44	8.04	7.85	-	-
pK[ML]	11.45	9.74	8.15	9.22	8.83	8.82	7.89	8.21
pK[$MH_{-1}L$]	-	10.77	-	10.14	10.14	9.93	-	-
pK[MHL_2]	-	-	-	-	-	-	-	-
pK [ML_2]	-	-	-	-	-	-	-	-
pK[$MH_{-1}L_2$]	-	-	10.91	-	-	-	9.51	-
pK[$MH_{-2}L_2$]	-	-	-	-	-	-	9.54	10.40
pK[$M_2H_7L_2$]	-	-	-	-	-	-	-	-
pK[$M_2H_6L_2$]	-	-	3.11	-	-	-	3.39	-
pK[$M_2H_5L_2$]	-	-	4.92	-	-	-	-	-
pK[$M_2H_4L_2$]	4.90	5.77	-	-	-	-	-	-
pK[$M_2H_3L_2$]	7.45	7.92	-	-	-	-	5.73	-
pK[M_2HL_3]	-	-	-	-	-	-	-	-

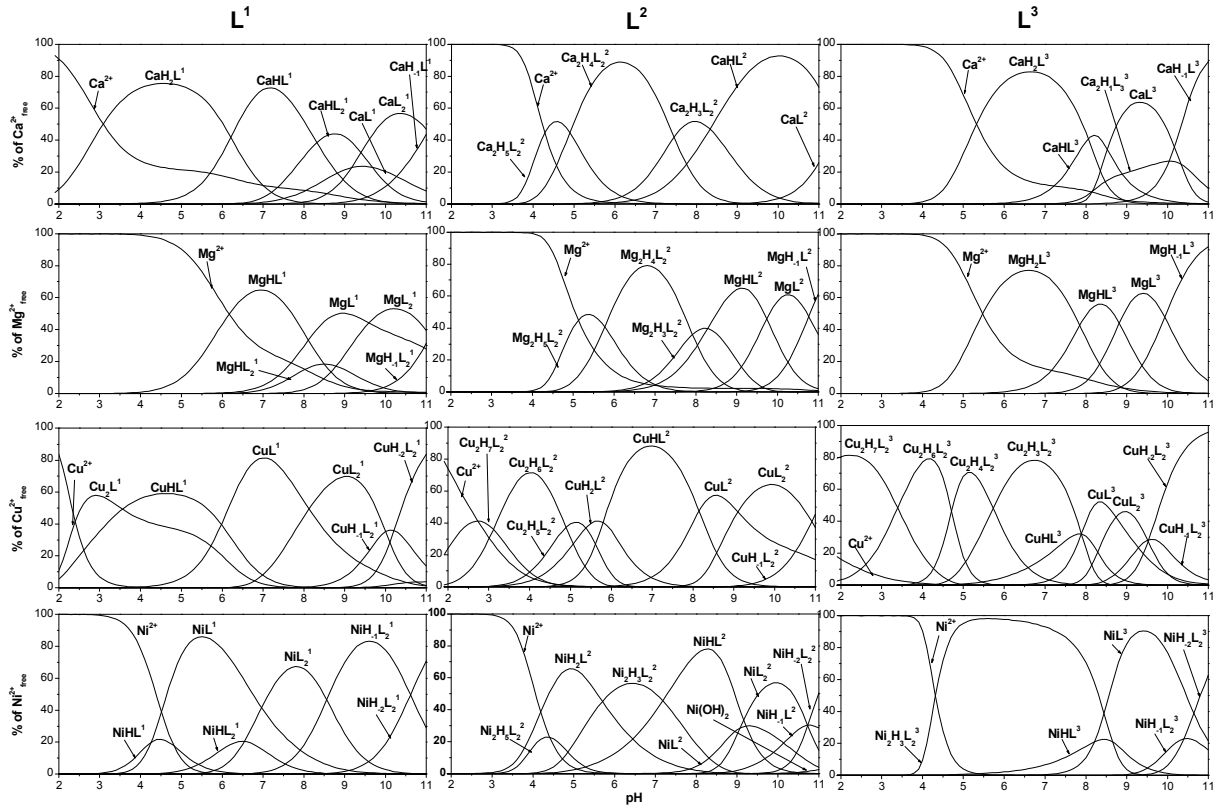

Fig. 3. Species distribution profiles for M^{2+} complexes of $L^{1,2,3}$ at 25°C and I = 0.1 M KCl, [L]=2×10^{-3}, [M]=1×10^{-3}.

View Article Online
DOI: 10.1039/C8NJ01158C

Table 4. Thermal transition parameters of studied systems (first binding site).

run	cell[a]	syringe[b]	pH[c]	*n*	K_{ITC} [M^{-1}]	ΔG_{ITC} [kJ mol^{-1}]	$\Delta H°_{ITC}$ [kJ mol^{-1}]	$\Delta S°_{ITC}$ [$Jmol^{-1}K^{-1}$]
L^1-Ca^{2+}	0.49	4.47	7.4	0.590	4.25^4	-26.41	0.95	91.80
L^2-Ca^{2+}	0.34	4.51	7.4	1.552	3.25^5	-31.45	-8.23	77.93
L^3- Ca^{2+}	0.24	4.47	7.4	3.147	4.35^4	-26.46	-2.41	80.72
L^1-Ca^{2+}	0.46	4.57	10.0	1.090	6.12^4	-15.73	-12.87	48.48
L^2- Ca^{2+}	0.46	4.57	10.0	1.808	2.95^5	-31.21	-4.07	91.08
L^3- Ca^{2+}	0.49	4.57	10.0	1.537	2.15^5	-18.82	-12.89	58.84
L^1- Mg^{2+}	0.38	4.48	7.4	1.521	9.38^3	-22.66	2.50	84.42
L^2- Mg^{2+}	0.35	4.48	7.4	2.050	5.86^4	-9.81	-19.34	26.42
L^3- Mg^{2+}	0.20	4.48	7.4	2.977	7.51^4	-27.82	-5.54	74.76
L^1- Mg^{2+}	0.44	4.47	10.0	1.345	6.02^4	-16.52	-11.95	51.44
L^2- Mg^{2+}	0.50	4.47	10.0	1.802	7.50^4	-27.82	-8.53	64.72
L^3- Mg^{2+}	-	-	10.0	-	-	-	-	-

[a]Initial concentrations of the ligands in the cell [mM]. [b]Initial concentrations of metal ions in the syringe [mM]. *n*: the molar ratio M^{2+}/L at which the inflection was observed on the titration curve. [c]Solvent details are described in Experimental section.

comparison of stability constants values does not give a straightforward answer for the question towards which metal ion a ligand binds more sufficient, due to several factors which overlap and influence the strength and formation yields of complexes e.g. concentrations, molar ratios, pH and metal-hydrolysis.[57]

Most likely only phosphonic moiety is involved into coordination of alkaline earth metal ions. UV-vis titrations of L^1 upon addition of Ca^{2+} and Mg^{2+} did not reveal any significant changes in wide pH range (data not shown) that suggests oxygen-only coordination. According to authors knowledge there is no examples of amino-BPs that coordinate towards Ca^{2+} and Mg^{2+} with an involvement of amine moiety. Those metal ions prefer pure O (phosphonate) coordination.[64]

In the solutions of L^2/Ca^{2+}, L^2/Mg^{2+} and L^3/Ca^{2+}, L^3/Mg^{2+} equimolar complexes were detected with no indication of biscomplexes (in contrast to respective L^1 systems), while polynuclear species are present for both studied ligands (Fig. 3, Table 3). In acidic pH range a presence of variously protonated $M_2H_nL_2$ (for L^2) and M_2L_3 complexes for Ca^{2+}/L^3 was proposed in potentiometric calculations and confirmed by ESI-MS for Mg^{2+}/L^2 system. These species (M_2L_2) co-exist of monomeric (ML) forms of complexes in solution (Table S2, Fig. S5, SI). Because the potentiometry is a method that is not able to distinguish between these two types of species, it causes the obtained species distributions for L^2 in acidic pH (Fig. 3) to be only a presumption.

In order to quantify the thermodynamics of the formation of Ca^{2+} and Mg^{2+} complexes, a direct determination of enthalpy binding change ($\Delta H°_{ITC}$) was applied by using isothermal titration calorimetry method (ITC). Measurements were performed in two pHs; 1) pH 7.4, chosen for biological reasons, and 2) pH 10.0, in which all phosphonic moieties are deprotonated. Titrations mode of ligand solution being an analyte and metal solution being a titrant was applied ($M^{2+}_{syringe} \rightarrow L_{cell}$). The results in the form of binding isotherms, that depend on stoichiometry (n), binding constant (K_{ITC}) and change on enthalpy ($\Delta H°_{ITC}$), are depicted in Fig. 4 and Fig. 5 with details of calculated fitting curves. Estimated values of K_{ITC}, n, $\Delta H°_{ITC}$ and $\Delta S°_{ITC}$ together with calculated Gibbs free energy ΔG_{ITC}, are given in Table 4.

Many classical interactions between ligand and metal ions are described by 'independent' model used to match the resulting binding isotherms that is based on 1 for 1 approach.[65] It was also applied to describe rarely performed ITC studies for metal-phosphonates interactions.[66] However, the interaction of BP with metal ions is more complex and in many cases it is not possible to use this simple approach. Titrations of zoledronic acid (1-hydroxy-2-(1*H*-imidazol-1-yl)ethylidene-1,1-bisphosphonate) with Ca^{2+},[67] up to date the only example of ITC studies of interactions of BPs with metal ions, were fitted using 'selective binding sites' model, because the isotherms have shown three inflections throughout the whole titration.[67] An existence of first endothermic event was followed by an exothermic one and a subsequent endothermic process. The authors attributed the results to a presence of CaL, CaL_2 and Ca_2L species that exist in pH dependent equilibrium. Isotherms obtained for studied herein systems; Ca^{2+}/L^1 in both studied pHs, $Ca^{2+}/L^{2,3}$, and Mg^{2+}/L^1 in pH 7.4 (Fig. 4, 5) showed one exothermic inflection point ($\Delta H°_{ITC}<0$) and could be fitted with 'independent site' model. Whereas Mg^{2+}/L^1, $Ca^{2+}/L^{2,3}$ in pH 10 and $Mg^{2+}/L^{2,3}$ in both pHs, clearly showed additional endothermic inflection (Fig. 4, 5). The latter curves have been fitted with 'multiple sites' model available in NanoAnalyze program, provided by the producer of the calorimeter.

In all studied cases the first (or the only existing) inflection can be assigned to metal ion binding (Table 4). Those are entropy driven, spontaneous processes ($\Delta G_{ITC}<0$). ΔG of binding of simple, non-amino-BPs with Ca^{2+} was previously shown to be ~29kJ/mol.[68] It stays in a good agreement with presented here data (except for Mg^{2+}/L^2 system for which ΔG_{ITC} is smaller) and confirms no additional support from a coordination of neither amino-group nor phosphonic function from the other side of the molecule (Table 4). For the systems into which 'multiple sites' models needed to be applied the second inflection was in all cases fitted with n~0.1-0.4 stoichiometry. Endothermic nature of those reactions does not allow to attribute this process to creation of new bonds ($\Delta H°_{ITC}>0$ for the second 'binding' site, see Fig. 4, 5). Rather a change in the water structure surrounding cation, i.e. the desolvation of water might be responsible for the observed thermal behavior with an endothermic character.[69] Nevertheless, the chemical nature of this inflection remains unclear since it might also be assigned to polymerization of unbound ligand individuals, to bonds breaking process or interactions with buffer molecules. At the same time neither cooperative effect nor competitive replacement type of interactions were detected.

View Article Online
DOI: 10.1039/C8NJ01158C

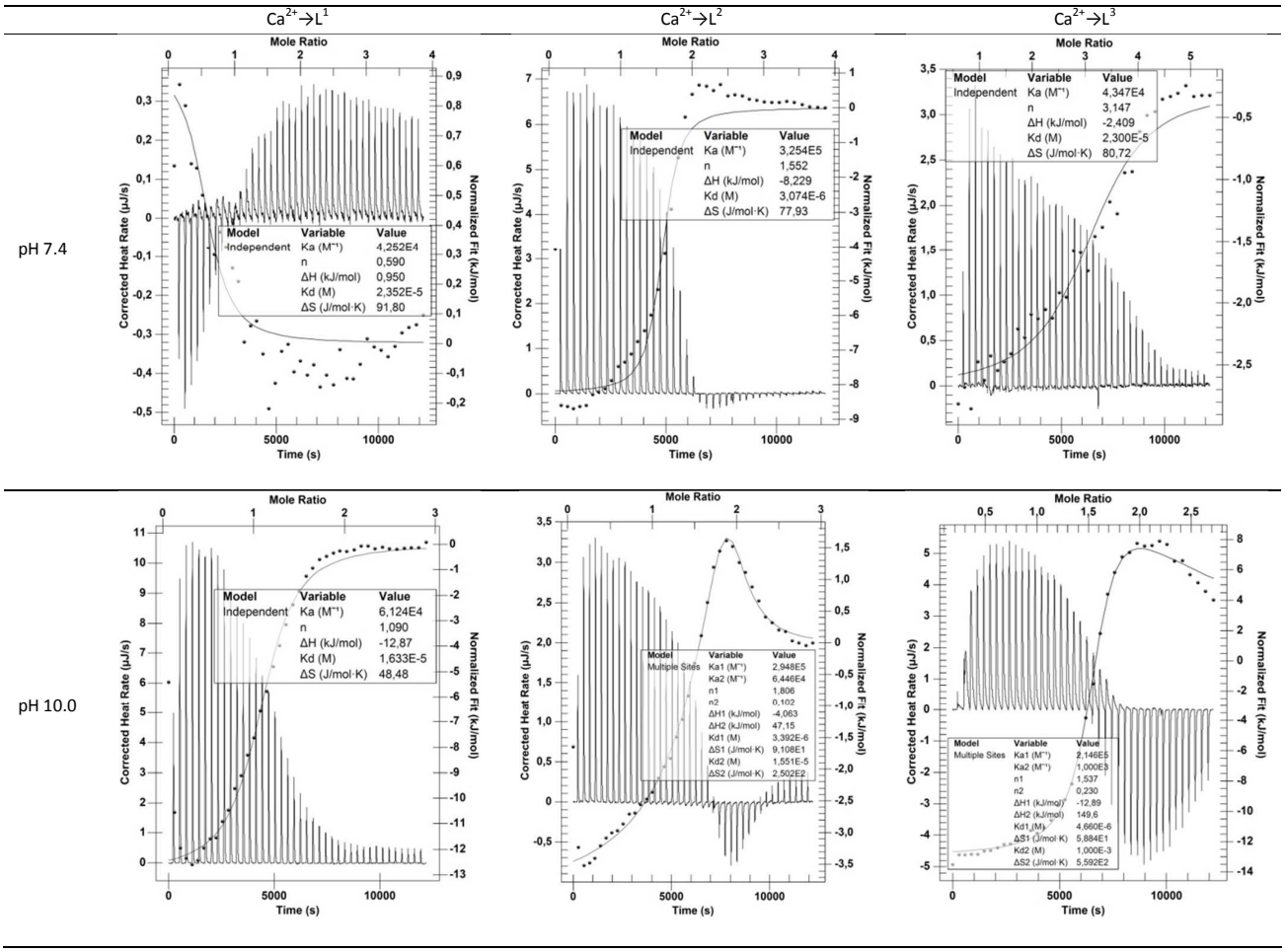

Fig. 4. ITC experiment of the titrations of Ca^{2+} →L^1, L^2, L^3 titrations at pH 7.4 and pH 10.0. Raw data overlaid with calculated models.

In order to give a comprehensive thermodynamic picture of studied systems and compare potentiometric data with calorimetric ones, the logarithms of conditional stability constants have been calculated ($\log K_c$) at fixed pH values and summarized in Table 5. Overall, the data stay in an agreement and are a good reflection of real binding strength, independent from the co-presence in the solution of different complex species. Yet due to the complex equilibrium in solutions, determined stoichiometry values (n) should be considered as approximate (Table 4). The fit of isotherms was carried out using standard program options assuming a binding of individuals in the solution with full saturation, which was not achieved for studied ligands, in particular below pH 7.4. Here, for almost all systems 'n' was estimated to be > 1, that would suggest the existence of M_nL complexes. However, they were not found for each case in ESI-MS studies. The affinity of the ligands expressed as $\log K_c$ value for both Ca^{2+} and Mg^{2+} ions rises with pH (see Table 4) most likely because above pH 10 all phosphonic groups are deprotonated and available for coordination. Dropping pH to the value of 7.4 drops this affinity by 1-2 logarithmic units.

Complexation of $Cu^{2+}$and Ni^{2+}. A coordination model for L^1/Ca^{2+} and L^1/Ni^{2+} does not differ significantly from the one of alkali earth metal ions, except the existence of Cu_2L^1 species in acidic pH and considerably higher (for approx. 5 logarithmic units) stability constants of formed complexes (Table 1, Fig. 3). ESI-MS spectra exhibit peaks which could be attributed to ML, ML_2 and M_2L (only for Cu^{2+} coordination). Furthermore, an existence of M_2L_2, M_3L_2 and M_3L_3 was detected (Table S2, SI).

Coordination for Cu^{2+} starts around pH 2, and Ni^{2+} ~ pH 3, what is confirmed by d-d absorption spectra of studied systems which maximum revealed blue-shifts at acidic pH (Fig. S2 and S3). Formation of MHL shifts maximum of absorption from 810 nm to 685 nm for Cu^{2+} and from 720 nm to 728 nm, and from 652 nm to 635 nm for Ni^{2+} (Table 6). Binding via oxygen atom only in analogues amino-BPs was causing d-d transition ~30 nm blue-shift only.[45] Here this significant change was four times bigger, so it lead us to an assumption that nitrogen atoms are involved in binding of the metal ion. Coordination in CuHL is most likely already implemented trough bidentate mode [N,O] with creation of unfavorable seven-membered ring. For Ni^{2+} such assumption is less probable since the change on the spectra correspond to ~ 20 nm shift, which rather are responsible for pure oxygen coordination in NiHL species. Since CuHL complex strongly overlaps with Cu_2L this notable shift for Cu^{2+}/L^1 can be partially attributed to the presence

DOI: 10.1039/C8NJ01158C

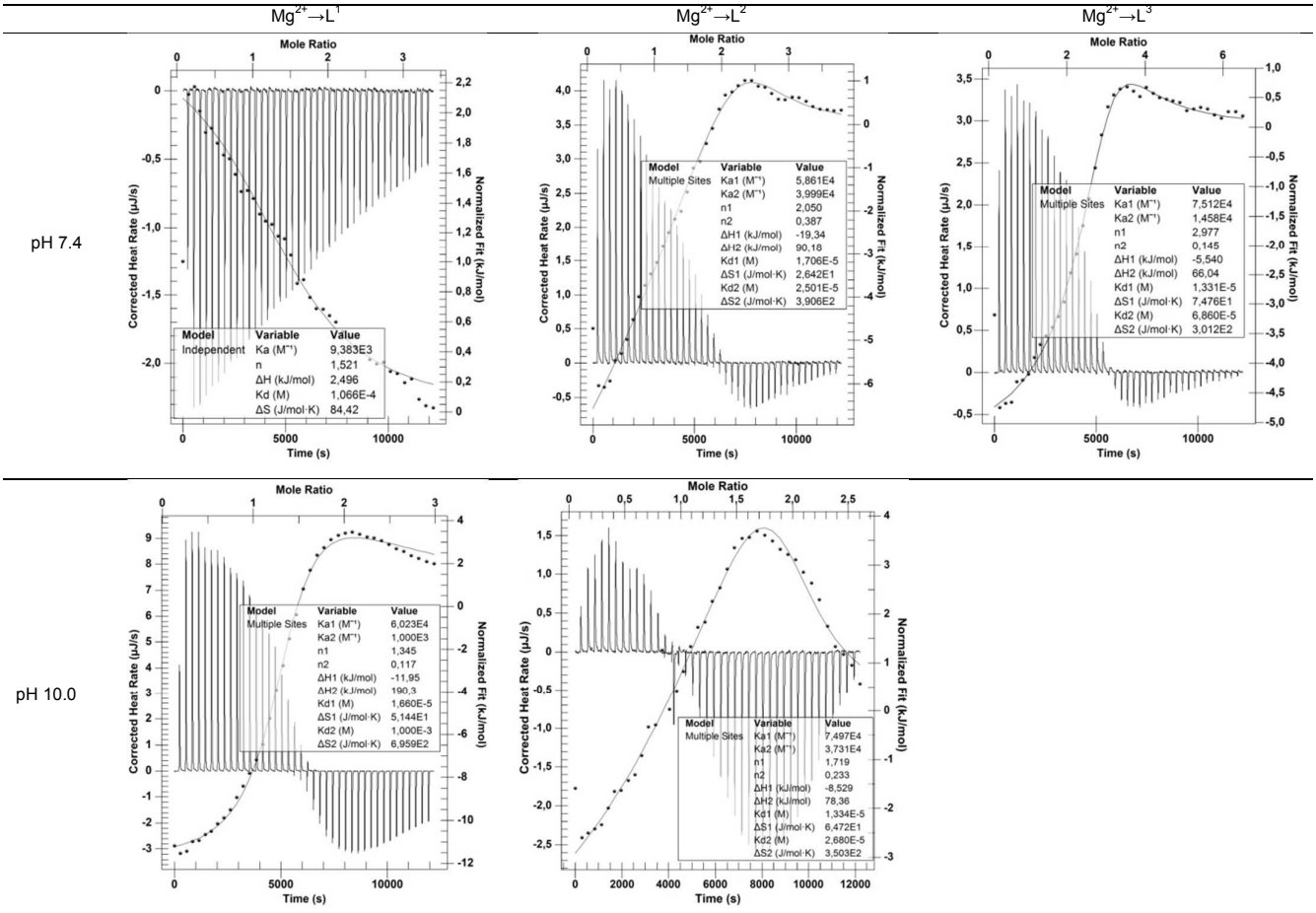

Fig. 5. ITC experiment of the titrations of Ca^{2+} →L^1, L^2, L^3 titrations at pH 7.4 and pH 10.0. Raw data overlaid with calculated models.

Table 5. Conditional stability constants (logK_c) for Ca^{2+} and Mg^{2+} complexes of studied ligands at selected pH values determined by potentiometry and ITC in 25°C.

M^{2+}/ligand	pH	logK_c (potentiometry[a])	logK_{ITC} (ITC[b])	match
Ca^{2+}→ **L¹**	7.4	4.00	4.63	+
Ca^{2+}→ **L²**	7.4	5.54	5.50	+
Ca^{2+}→ **L³**	7.4	3.88	4.64	+
Ca^{2+}→ **L¹**	10.0	5.92	4.78	~
Ca^{2+}→ **L²**	10.0	5.85	5.47	+
Ca^{2+}→ **L³**	10.0	5.11	5.33	+
Mg^{2+}→ **L¹**	7.4	3.50	3.97	+
Mg^{2+}→ **L²**	7.4	4.02	4.32	+
Mg^{2+}→ **L³**	7.4	3.75	4.76	~
Mg^{2+}→ **L¹**	10.0	5.76	4.79	~
Mg^{2+}→ **L²**	10.0	4.87	4.77	+
Mg^{2+}→ **L³**	10.0	5.17	nd	

[a]Obtained by Hyss2009 based on traditional approach introduced by G.Schwarzenbach,[70] defined as $K_c=[M^{2+}]_{bound\ to\ L}/[M^{2+}]_{not\ bound\ to\ L}\times[M^{2+}]_{not\ bound\ to\ M2+}$, based on experimental logβ values (under concentration conditions: $[M^{2+}]=2.0\times10^{-6}$-$1.0\times10^{-3}$, $[L]=2.0\times10^{-3}$ and fixed pH value). [b]Based on direct ITC result of K_{ITC} (Fig. 4, 5, Table 4).

of a complex in which one ligand binds two metal ions. Nevertheless, the involvement of NH_3^+ throughout a whole pH range is rather unfavorable due to steric reasons. Primary amine was reported to be involved in charge-assisted hydrogen-bonding which stabilized the complex structure, but its binding to either Cu^{2+}[58] or Ni^{2+}[61] was excluded in solid state. Possibly as soon as phosphonic groups are deprotonated the coordination with unfavourable geometry is replaced by [O,O] bidentate, purely

View Article Online
DOI: 10.1039/C8NJ01158C

Table 6. Spectroscopic characteristics of Cu^{2+} and Ni^{2+} complexes.

Ligand	Species	UV-vis[a] parameters		
		pH	λ(nm)	ε (M^{-1} cm^{-1})
L^1	$[Cu_2L]$	2.0	737	16
	$[CuHL]^b$	3.0	685	35
	$[CuL]$	7.0	701	49
	$[CuL_2]^b$	9.0	707	58
	$[CuH_{-1}L_2]$	10.0	702	58
	$[CuH_{-2}L_2]^b$	11.0	694	61
L^2	$[CuH_2L]^b$	5.5	755	31
	$[CuHL]^b$	7.0	702	40
	$[CuL]^b$	8.5	658	44
	$[CuL_2]^b$	10.0	647	46
	$[CuH_{-1}L_2]$	11.0	650	46
	$[Cu_2H_nL_2]$	2.0-5.0	nd	-
L^3	$[CuHL]$	7.0	nd	-
	$[CuL]$	8.5	nd	-
	$[CuL_2]$	9.0	nd	-
	$[CuH_{-1}L_2]$	9.5	nd	-
	$[CuH_{-2}L_2]$	11.0	606	46
	$[Cu_2H_nL_2]$	2.0-8.0	nd	-
L^1	$[NiHL]^b$	4.6	728(sh), 635, 384	5.4, 6.1, 11
	$[NiL]^b$	6.0	735(sh), 644, 383	6.9, 9, 15
	$[NiHL_2]$	6.5	nd	-
	$[NiL_2]^b$	8.1	651, 386	10, 22
	$[NiH_{-1}L_2]^b$	9.5	648, 384	15, 34
	$[NiH_{-2}L_2]^b$	10.9	644, 379	18, 47
L^2	$[NiH_2L]$	4.8	nd	-
	$[NiHL]$	8.0	755, 679, 408	4.9, 4.8, 12.5
	$[NiL]$	9.0	nd	-
	$[NiH_{-1}L]$	10.5	nd	-
	$[NiL_2]$	10.0	755(sh), 683, 405	5, 6, 15
	$[NiH_{-2}L_2]$	11.0	nd	-
	$[Ni_2H_nL_2]$	3.0-6.5	nd	-
L^3	$[NiHL]$	8.5	nd	-
	$[NiL]$	9.5	nd	-
	$[NiH_{-1}L_2]$	10.5	nd	-
	$[NiH_{-2}L_2]$	11.0	749, 685, 406	5.6, 5.5, 16
	$[Ni_2H_nL_2]$	6.0	nd	-

[a]d-d. For comparison; $[Cu(H_2O)_6]^{2+}$, λ [nm](ε [M^{-1} cm^{-1}])=810(17), $[Ni(H_2O)_6]^{2+}$, 720(3.3), 652(3), 393(6.4), under the same concentration conditions as measured systems. The data reflect optical properties of solutions in which the given forms are major species. Sh=shoulder. Nd=not detected. [b] Stability constants of marked species calculated in *HypSpec2014* based on spectrophotometric titrations are given in Table S1, SI.

phosphonic with six-membered rings or [N,O] mixed coordination mode with a participation of NH^+R. Rising pH up to 7 leads to creation of CuL which causes red-shift of maximum of d-d band from 685 nm to 701 nm. Final deprotonation of phosphonic function and creation of [N,O,O] tridentate favored by other amino-BPs systems[45] coordination might be responsible for this spectral shift. Further pH rise leads to the formation of CuL_2. The energy of d-d transition for CuL_2 complex equals to λ=707nm and ε=58(M^{-1} cm^{-1}) and is higher in relation to the d-d absorption band of CuL. No significant shift suggests an involvement in binding of a second ligand oxygens only. Above pH 10 the band blue-shifts slightly from 707 nm to 694 nm. For Ni^{2+}/L^1 the changes do not exceed ~ 5 nm. Species distribution diagrams show in this pH region a formation of $MH_{-1}L_2$ [$M(OH)L_2$] and $MH_{-2}L_2$ [$M(OH)_2L_2$] hydroxy-complexes (p*K* range: 8.61-10.56). Calculations based on UV-vis titrations of the Cu^{2+}/L^1 and Ni^{2+}/L^1 systems confirms proposed model and calculated stability constants are given in Table S1, SI.

Cu^{2+} and Ni^{2+} speciation profiles for L^2 and L^3 are depicted on Fig. 3 and are comparable. Coordination of Cu^{2+} is more favourable and starts for both ligands below pH 2, for Ni^{2+} ~ pH 3.5 with a formation of oligomeric complexes of M_2L_2. stoichiometry (Table 3) Their presence was confirmed by ESI-MS studies for Cu^{2+}/L^2 and Ni^{2+}/L^2 systems (Table S2, Fig. S5, SI). M_2L_2 complexes coexist in the solution with ML species in acidic pH (Fig. 3). Since for Cu^{2+}/L^2 and Ni^{2+}/L^2 systems upon applying 1:1 molar ratio in spectroscopic studies revealed the presence of opalescence (below pH 5), we assume that the oligomers aggregate in solution and create precipitation. It should be added that polymerization of partly deprotonated ligands may occur in parallel and probably have an additional effect on precipitation. Precipitation in an almost whole pH range permitted to obtain spectroscopic data for Cu^{2+}/L^3 and Ni^{2+}/L^3 (Table 6, Fig. S3). When rising pH up to 5 in case of Cu^{2+}/L^2 and up to 7 for Ni^{2+}/L^2, only equimolar species and biscomplexes are present in the solution. Identified by ESI-MS species are as following: $NiL^{2,3}$, CuL^3, $CuL^2{}_2$ and $CuL^2{}_3$.

First formed equimolar complex is MH_2L which causes blue-shifting of maximum of d-d band from 810 nm for $Cu^{2+}{}_{aqua}$ to 755 nm. For Ni^{2+} a spectral change is reflected in ~ 20 nm shift (Table 6). Coordination of M^{2+} in MHL can be therefore attributed to simple bidentate coordination [O,O].[60] Creation of CuHL most likely corresponds to deprotonation only of second bisphopshonic function (pK=5.80 for Cu^{2+}/L^2 and 6.44 for Ni^{2+}/L^2). In pH range 7-10 the d-d transition band of Cu^{2+}/L^2 system shifts significantly from 755 nm to 647 nm and suggests an involvement of nitrogen atom in coordination [N,O,O] in CuL and later on 2× [N,O,O] in CuL_2, as for single-amino-BPs studied previously.[45] Further deprotonation to hydrolytic species (pK 10-77-10.91) can be assign to $H_2O \rightarrow OH^-$ process. However, since almost no changes were detected on Ni^{2+}/L^2 system above pH 8 (see Fig. S3, SI) we assume that the involvement of NH^+R in Ni^{2+} coordination is rather not possible and the coordination mode remain purely oxygen one.[63]

Absorption spectra show that all Cu^{2+} and Ni^{2+} complexes of studied ligands are of octahedral or pseudo-octahedral geometry.

Liphophilicity measurements

BPs are characterized as highly hydrophilic compounds in general. This is the reason for their low bioavailability when administered as drugs and one of a serious problems associated with the administration of high doses of BPs during treatment. In order to estimate lipophilicity of studied compounds, shake flask method was applied.[71] A partition coefficient ($logP_{o/w}$), that provides a measure by which to assess the ability of a drug candidate to be absorbed across an intestinal membrane, was determined experimentally for free ligands and their Ca^{2+} complexes. The results are presented in Table 7 in comparison to alendronate (4-amino-1-hydroxybutyl-1,1-bisphosphonate), routinely used drug for osteoporosis treatment. All ligands exhibit $logP_{o/w}$ values which indicate a hydrophilic character, as expected, notwithstanding - smaller than alendronate. An increase of lipophilicity upon binding via polar functions to metal ion is observed for Ca^{2+} complexes, what most likely would be reflected in higher intestinal uptake of complexes in comparison to free ligands.

View Article Online
DOI: 10.1039/C8NJ01158C
NJC ARTICLE

Table 7. Experimentally Determined log$P_{o/w}$ Values.[a]

Compound	log $P_{o/w}$ (L)	log $P_{o/w}$ (Ca^{2+}/L, 1:1)	log $P_{o/w}$ (Ca^{2+}/L, 1:2)
L^1	-1.27 ± 0.3	-0.53 ± 0.3	-0.24 ± 0.3
L^2	-2.00 ± 0.3	-0.88 ± 0.3	-0.84 ± 0.3
L^3	-2.43 ± 0.3	-0.77 ± 0.3	-1.28 ± 0.3
incadronate	nd	nd	nd
alendronate	-4.49[72,73][b]		

[a]Shake-flask method; $P_{o/w} = [\ ]_{1\text{-octanol}}/[\ ]_{HEPES}$; pH 7.4; 25°C, concentration determined by UV-vis absorption. Incadronate log$P_{o/w}$ values cannot be measured due to a lack of spectra in UV-vis range.[b]calculated

***In vitro* anticancer activity**

Colon adenocarcinoma and melanoma skin cancer are the most common malignancy throughout the world. Both cell lines (HT29 and A375) are a well-established model of colon and skin cancer, which preferentially metastasizes to bone.[74] *In vitro* anticancer activities of the ligands and Ca^{2+} and Mg^{2+} complexes were evaluated in melanoma A375 cells and human colon adenocarcinoma HT29 cell by the MTT assay. Incadronate was used for reference purposes. Representative dose–response curves are shown in Fig. S8, SI. Ligands; L^1 and incadronate significantly suppressed cell growth in both A375 and HT29 cell lines, whereas L^2 and L^3 had weaker effects. The resulting half minimal inhibitory concentration (IC_{50}) values were displayed in Table 8. All of the compounds exhibited cytotoxic activity at tested concentrations (IC_{50} > 600 μM). Notably, L^1 and incadronate gave rise to IC_{50} values of less than 350 μM and 450 μM in a case of A375 and HT29 cell lines, respectively. Among all tested Ca^{2+} and Mg^{2+} complexes of L^1 and incadronate, the species showed higher cytotoxicity on A375 and HT29 cells than the free ligands. Compounds L^2 and L^3 containing Ca^{2+} and Mg^{2+} showed decrease cytotoxicity in proliferation to cell lines. As a general observation, the complexes of single-amino-BP showed higher effectiveness against both the cell lines than the respective complexes of double-amino-BPs. Although the mechanism of the antitumor activity exhibited by these ligands and their complexes remains unknown, we tentatively suppose that they may directly induce apoptosis in cancer cell lines, as previously reported for similar compounds.[75,76]

Table 8. Anti-proliferative activity of studied ligands with or without Ca^{2+} or Mg^{2+} against melanoma A375 cells and adenocarcinoma HT29 cells.

Compounds/complexes	IC_{50} [μM]	
	A375	HT29
L^1	349.24±3.42	435.19±3.26
L^1-Ca^{2+}	215.28±2.04	338.91±2.47
L^1-Mg^{2+}	313.31±2.11	410.78±2.02
L^2	527.25±2.88	486.16±7.22
L^2-Ca^{2+}	539.46±4.91	519.75±0.86
L^2-Mg^{2+}	543.28±1.85	540.55±4.21
L^3	577.36±5.21	541.55±3.21
L^3-Ca^{2+}	603.61±1.75	587.02±2.19
L^3-Mg^{2+}	647.53±0.32	695.31±4.83
incadronate	328.03±2.64	423.16±1.49
Incadronate-Ca^{2+}	243.92±1.38	282.61±5.29
Incadronate-Mg^{2+}	273.42±5.71	382.50±2.75

The most abundant species under conditions of IC_{50} in pH 7.4 are given in Fig. S6, SI, that depicts recalculated distribution species diagrams in narrow pH range. The diagrams indicate complex equilibrium out of which one active species cannot be clearly pointed out. A majority of cases exhibits coexistence of protonated species of complexes with protonated forms of free ligands.

Conclusions

In this study combined potentiometric, ESI-MS, spectroscopic and calorimetric studies allowed us to investigate complex-formation abilities of three amino-BPs based on cyclohexane backbone: one single-amino-BPs (equipped in one bisphosphonic moiety) and two double-amino-BPs (equipped in two bisphosphonic moieties) in complexation of Ca^{2+}, Mg^{2+}, Cu^{2+} and Ni^{2+} ions in aqueous solution. Both ligands and their complexes were tested in terms of cytotoxic activity with respect to two cell lines (human melanoma A375 and human colorectal adenocarcinoma HT29) and half minimal inhibitory concentrations (IC_{50}) were determined.

Complex equilibria in solution consist of equimolar, biscomplex and oligomeric complexes, which is a typical feature for amino-BPs. In a coordination of Ca^{2+}, Mg^{2+} and probably Ni^{2+}, the amino groups of studied ligands are not involved, whereas in the case of Cu^{2+}, a participation of both: NH_3^+ (for L^1, up to pH 7) and NH^+R group (for all ligands) is highly probable. L^1, L^2 and L^3 bind biogenic metal ions upon spontaneous, exothermic reaction that are entropy driven processes and create stabile complexes in broad pH range. Stability constants of ML complexes fall into well-known rank: $\log\beta_{CuL} > \log\beta_{NiL} >> \log\beta_{MgL} \sim \log\beta_{CaL}$ and the magnitude of order of logβs is consistent with literature data for single-amino-BPs, that confirms no participation of second BP moiety in binding of one metal ion. Estimated via potentiometry (logK_c) and isothermal titration calorimetry (logK_{ITC}) independent conditional stability constants for pH 7.4 and pH 10.0 stay in a good agreement.

Ca^{2+} and Mg^{2+} complexes of L^1 as well as incadronate showed higher inhibitory rate than their free ligands against A375 and HT29 cell lines. However, it was impossible to indicate which complex is active, because in the conditions of biological measurements the equilibrium consist both: complexed and unbound ligand molecules. In comparison, L^2 and L^3 complexes showed slight decrease of cytotoxicity upon coordination against both cell lines.

Incorporation of cyclohexane backbone increased the liphophilicity of studied ligands, which is desirable for newly designed ligands that are intended to potentially act in direct or indirect way as drugs or building-blocks for drugs-related materials Furthermore, since being equipped in a second donor function, apart from bisphosphonic one, did not change the complexation abilities of studied ligands in comparison to literature examples of single-amino-BP it opens new route of thinking for such compounds to use this second function as an anchor for a different molecule.

Experimental Section

Chemicals

All solvents and reagents were purchased from commercial suppliers, were of analytical grade and were used without further purification. Unless otherwise specified, solvents were removed with a rotary evaporator. The ^{1}H-, ^{31}P- and ^{13}C-NMR spectroscopic

View Article Online
DOI: 10.1039/C8NJ01158C

experiments were performed on a Bruker Avance II Ultrashield Plus (Bruker, Rheinstetten, Germany) operating at 600.58 MHz (^{1}H), 243.12 MHz (^{31}P{1H}) and 151.016 MHz (1^3C). Measurements were made in solutions of D_2O + NaOD at 300 K, and all solvents were supplied by ARMAR AG (Dottingen, Switzerland). Chemical shifts are reported in ppm relative to TMS and 85% H_3PO_4, used as external standards, and coupling constants are reported in Hz. Melting points were determined on an SRS Melting Point Apparatus OptiMelt MPA 100 (Stanford Research Systems, Sunnyvale, CA, USA) and are reported uncorrected. Mass spectra were recorded at the Faculty of Chemistry, Wroclaw University of Science and Technology using a Waters LCT Premier XE mass spectrometer (method of electrospray ionization, ESI) (Waters, Milford, MA, USA).

General procedure of the synthesis of aminomethylenebisphosphonic acid (L^1) and bisaminomethylenebisphosphonic acids (L^2, L^3)

Diamine (0.03 mol) and the appropriate amounts of diethyl phosphite (0.126 mol, 16.32mL) and triethyl orthoformate (0.063 mol, 4.4mL) were were heated and simultaneously stirred at a temperature of ~130 °C on a heating plate (125 °C in the reaction medium) of a Radley's Carousel apparatus overnight (15 h). The mixture was cooled, and the volatile components were removed using a rotary evaporator. The resulting mixture was dissolved in ethyl acetate (100 mL) and purified by washing with water (100 mL), saturated sodium chloride solution (100 mL) and again with water (100 mL). The solution was dried over anhydrous $MgSO_4$, and the solvent was evaporated under vacuum. The obtained ester (0.030 mol) was refluxed for 15 h (overnight) in 40 ml 6 N aqueous hydrochloric acid solution. After cooling, the volatile components were removed using a rotary evaporator, and the resulting oil was dissolved in minimal amount of water (40-50 mL), discolored with activated charcoal and purified by crystallization from water–ethanol mixture (80/20 v/v). The impure product was mixed with water for few days until the dissolution of impurities was observed and then was filtered and washed with distilled water and dried in vacuum.

Synthesis of L^1. *Cyclohexane-1-amino-2-aminomethylene-bisphosphonic acid (L^1)* was obtained as a white solid; yield: 64%; mp 235-236^{0}C; ^{31}P-NMR (243.12 MHz, D_2O+NaOD, ppm) δ = 17.73 (AB system, *J*=17.73Hz); ^{1}H-NMR (600.58 MHz, D_2O+NaOD, ppm) δ = 0.82 (q_{br}, *J*=11.50Hz, 1H), 1.01 (m, 1H), 1.08-1.12 (m, 2H), 1.49-1.54 (m, 2H), 1.66 (d, *J*=12.55Hz, 1H), 1.99 (d, *J*=12.76HZ, 1H), 2.21-2.26 (m, 1H), 2.44-2.48 (m, 1H), 2.67 (d, *J*=16.88Hz, C<u>H</u>P); 2.71 (d, *J*=17.17, C<u>H</u>P); ^{13}C-NMR (151.02 MHz, D2O+NaOD, δ = 24.51, 24.73, 30.57, 33.68, 55.43, 56.26 (d, *J*=123.06Hz, CP), 57.13 (d, *J*=124.50Hz, CP);[35,77] HRMS (TOF MS ESI); [M-H]$^-$ Calcd for $C_7H_{18}N_2O_6P_2$: 287.0562; found: 287.0511.

Synthesis of L^2. *Cyclohexane-1,3-di(aminomethylenebisphosphonic) acid* (L^2) was obtained as a white solid; yield:51%; mp 269-270 ^{0}C; ^{31}P-NMR (243.13 MHz, D_2O+NaOD, ppm) δ = 17.54&17.78; ^{1}H-NMR (600.58 MHz, D_2O+NaOD, ppm) δ = 1.18-1.23 (m, 2H, CH_2), 1.31-1.39 (m, 2H, CH_2), 1.46-1.54 (m, 4H, CH_2), 2.67(t, 2H, *J*=16.77Hz, C<u>H</u>P_2), 3.09-3.16 (m, 2H, CHN); ^{13}C-NMR (151.02 MHz, D_2O+NaOD, δ = 18.88, 28.50, 37.27, 51.52, 54.82 (t, *J*=127.97Hz, CHP_2);[35,77] HRMS (TOF MS ESI); [M-H]$^-$ Calcd for $C_8H_{22}N_2O_{12}P_4$: 461.0045; found: 461.0032.

Synthesis of L^3. *(trans)-Cyclohexane-1,4-di(aminomethylene-bisphosphonic) acid* (L^3) was obtained as a white solid; yield: 52%; mp 243 ^{0}C; ^{31}P-NMR (243.12 MHz, D_2O+NaOD, ppm) δ = 18.50; ^{1}H-NMR (600.58 MHz, D_2O+NaOD, ppm) δ =1.31-1.41 (m, 4H, CH_2), 2.14-2.23 (m, 4H, CH_2), 2.98 (t, *J*=16.10Hz, 2H, CHP), 3.38-3.47 (m, 2H, CHN); ^{13}C-NMR (151.02 MHz, D_2O+NaOD, δ = 27.51 (CH_2), 55.35 (t, *J*=116.20Hz, CHP_2), 56.22 (CHN);[35,36,77] HRMS (TOF MS ESI); [M-H]$^-$ Calcd for $C_8H_{22}N_2O_{12}P_4$: 461.0045; found: 461.0047.

Synthesis of incadronate. *N-(cycloheptyl)aminomethylene-bisphosphonic acid (Incadronate)* was obtained as a white solid; yield: 67%. Cycloheksylamine (0.03 mol, 3.39 g), triethyl orthoformate (0.033 mol, 5.30 mL) and diethyl phosphite (0.066 mol, 8.52 mL) were heated and simultaneously stirred at a temperature of ~130 °C on a heating plate (125°C in the reaction medium) of a Radley's Carousel apparatus overnight (15 h, Radleys, Essex, UK). The mixture was cooled, and the volatile components were removed using a rotary evaporator. The resulting mixture was dissolved in ethyl acetate (100 mL) and purified by washing with water (100 mL), saturated sodium chloride solution (100 mL) and again with water (100 mL). The solution was dried over anhydrous $MgSO_4$, and the solvent was evaporated under vacuum. Boiling in 20 mL of 6 N hydrochloric acid for 12 h hydrolysed the resulting crude reaction product. After cooling, the volatile components were removed using a rotary evaporator, and the resulting oil was dissolved in minimal amount of water (30 mL), discolored with activated charcoal and purified by crystallization from hot water/ethanol mixture. Mp 249-250°C; ^{31}P-NMR (243.12 MHz, D_2O+NaOD, ppm) δ =8.03; ^{1}H-NMR (600.58 MHz, D_2O+NaOD, ppm) δ =1.49-1.63 (m, 6H, CH_2), 1.67-1.80 (m, 4H, CH_2), 2.11-2.21 (m, 2H, CH_2), 3.59 (t, *J*=18.23Hz, 1H, CHP_2), 3.66-3.74 (m, 1H, CHN); ^{13}C-NMR (151.02 MHz, D_2O+NaOD) δ= 24.49, 25.42, 31.46, 54.71 (t, *J*=124.39Hz, CHP_2), 56.14 (CHN);[45,77,78] HRMS (TOF MS ESI); [M-H]- Calcd for $C_8H_{19}NO_6P_2$: 286.0609; found: 286.0597.

The studied ligands are well soluble in aqueous solutions in the range of concentrations used in the experiments (details below).

Potentiometry

The chemicals were commercial products of reagent grade and were used without further purification. Solutions were prepared with bidistilled water which were flushed with Ar to exclude CO_2. The ionic strength was fixed at *I* = 0.1 M with KCl (POCh). The titrations were performed using a Metrohm 809 Titrando system equipped in combined glass electrode (Metrohm 6.0224.100) which was calibrated daily in hydrogen concentrations using HCl (Merck) (~0.004M) according to the procedure of Irving *et al.*[79] Alkali, CO_2-free 0.1029 M KOH solution (POCh) was added from a Metrohm 800 Dosino auto burette. The purity and exact concentration of the ligand were determined by the method of Gran.[80] The stock solutions of metal ions were prepared by dissolving the appropriate amount of chlorides in aqueous HCl solution. All the titrations were carried out on 2.0 ml samples in a thermostatted cell at 25±0.2°C

View Article Online
DOI: 10.1039/C8NJ01158C

under a stream of Ar. *HYPERQUAD2013*[81] computer program that use non-linear least-squares methods[82] was applied to calculate the stability constants. The results were obtained in the form of concentration overall stability constants $\beta_{pqr} = [M_pH_qL_r]/[M]^p[H]^q[L]^r$, where M stands for metal. H is proton and L the deprotonated form of the ligand. Triplicate titrations of the free ligand and the complexes were carried out at metal to ligand ratios 1:1.1, 1:2, 1:3 and 1:4. Opalescence occurred in 1:1.1 solution of L^2 with Cu^{2+} and Ni^{2+} in acidic pH. The precipitation in whole pH range was present in 1:1.1 solutions of L^3 with Cu^{2+} and Ni^{2+}. The titrations with opalescence or precipitations were excluded from calculations and higher molar ratios were applicated. The ligand concentration was 1.0×10^{-3} mol dm^{-3} in all titrations. The distribution curves of the protonated species of ligands as a function of pH were calculated using *HySS2009* program.[83]

Spectrophotometric measurements and combined potentiometric/spectrophotometric measurements.

Absorption spectra in combined potentiometric and UV-vis titrations were collected using Varian Cary 50 spectrophotometer equipped with immersion probe made of Quartz SUPRAZIL®300 and removable light path tip with 1cm optical path (type 665.622) for Cu^{2+} and Ni^{2+} complexes. The initial pH of 10 ml samples prepared in 0.1M (KCl) ionic strength was adjusted to be acidic and the titration of the solution was carried out by addition of known KOH volumes dosed by Metrohm 809 Titrando system. Special care was taken to ensure that complete equilibration was attained before collecting the spectra. The spectral deconvolutions were refined using the least squares fitting program *HypSpec2014*.[84] Factor analysis by the *HypSpec* software was implemented to characterize the number of species present in the solution. The concentration of ligands was $2.0\text{-}3.0\times10^{-3}$M for Cu^{2+} measurements and $3.0\text{-}5.0\times10^{-3}$M for Ni^{2+}. For L^1 molar ratio M^{2+}:L was kept 1:2 and for L^2 and L^3 1:1 since while having 1:2 (and 1:3) solutions disclosed slight precipitation. For L^3 for both metal ions it was possible to record only few spectra (Fig. S2 and S3) due to a precipitation under applied conditions, lowering concentration to 1.0×10^{-3}M as it was used for potentiometric studies caused the spectra to be in the range of noise. Experimental errors on λ_{max}=±2nm and ε=±5%.

Absorption spectra for liphophilicity studies were collected using Hitachi HALO DB-20 double beam spectrophotometr (U-2800), using quartz Hellma cuvettes.

Mass spectrometry

All ESI-MS experiments were performed on a compact™ mass spectrometer (Bruker Daltonics, Bremen, Germany) equipped with standard ESI source. The instruments were operated in the positive-ion mode and calibrated with the Tunemix™ mixture (Agilent Technologies. Palo Alto. CA. USA) in a quadratic method. Spectra were recorded for samples dissolved in MeOH/H_2O 50/50 mixture with M:L molar ratio 1:1 and 1:2 (pH~5, lowered by HCl and pH~7-8, raised up by KOH, rising pH up to 10 in each case caused a significant deterioration of the spectrum) and heated up to 40°C for 15 min prior to the experiment. In case when a precipitation was formed, the solids were filtered off and the clear solution was measured. Strong precipitation was observed regardless of concentrations, molar ratios and pH for L^3 with all studied metal ions, it reflected with no results for L^3/Ca^{2+}, Mg^{2+} systems (after filtration). Except for Cu^{2+}/L^1 system (to which both data are given in Table S1, SI) no significant differences between different molar ratios were noticed. Analyte solutions (70 µl) were introduced at a flow rate of 3 µl/min. The instrument parameters were as follows; scan range: 50–3000 m/z, drying gas: nitrogen, flow rate: 4.0 L/min, temperature: 200 °C and potential between the spray needle and the orifice: 4.0 kV. For MS spectra analysis a Bruker Compass DataAnalysis 4.2 software was used. A sophisticated numerical annotation procedure (SNAP) algorithm was used for finding peaks. Relative intensities (Table S1 and S2) were read directly from the MS spectra in the DataAnalysis 4.2 program. The Supplementary Information contain raw MS spectra with intensities on the y-axis and isotopic patterns enlargements for the main species present.

Isothermal titration calorimetry

ITC experiments were carried out using a Nano ITC calorimeter (TA Instruments) with a standard volume of 1.0 ml cell at 25°C. In a typical experiment the solution of ligand (0.24-0.50mM; in buffer) was placed in the cell and the solution of; Ca^{2+} (4.47-4.57mM, in buffer) or Mg^{2+} (4.47-4.48mM, in buffer) was taken up in a 250 µL injection syringe. The concentration of buffers (HEPES pH 7.4, CAPS pH 10.0) was 100mM. pH of each sample was measured before and after the experiment to be sure of keeping it constant. Each sample was degassed prior the titration for 5 minutes. The total number of 40 injections, 6 µL each were added after the calorimeter finalized the primary equilibration, with 300s apart. The stirring rate was 300rpm. The calorimeter was operated using the Nano ITC Run software and all the data obtained were analyzed with the NanoAnalyze v. 3.1.2 program. 'Independent' or 'multiple sites' models were used to evaluate the results obtained and the control experiments were performed in each case; the enthalpies of reagents dilution were subtracted from the enthalpies of binding processes. Each ITC data was collected by two independent measurements and reproducible data was employed. Standard deviation fit of the data is provided in the Supplementary Information (Fig. S7, SI).

Lipophilicity measurements

The shake-flask method was used to experimentally determine the log $P_{o/w}$ values for studied ligands and their calcium complexes. The aqueous (50mM HEPES, pH 7.4 and I_{KCl}=0.16M, 25°C) and 1-octanol solvents were used in the experiment. 0.750ml of 1-octanol and 0.75ml of 1mM solution of studied ligand or complex (in molar ratio 1:1 and 1:2, [L]=2×10^{-3}M) were mixed together. The samples were vortexed (~2min), shaked manually (~2min) and centrifuged (~1min, 5000 rpm). The layers were separated and measured by UV-vis spectroscopy, applying the Beer-Lambert law to determine the ligand concentration in analyzed layer (ε i λ_{max} are given in Table S3, SI). Measurements were run in triplicate. Incadronates' lipophilicity could not be measured due to a lack of spectra in measured range.

View Article Online
DOI: 10.1039/C8NJ01158C

Cell lines and culture conditions

The human cancer cell lines, melanoma (A375) and colon adenocarcinoma cells (HT29) were used for *in vitro* screening experiments. A375 melanoma (ATCC CRL-1619) cells and colon adenocarcinoma cell line HT29 were obtained from Dr. Dorota Nowak and Dr. Elżbieta Gocek (University of Wroclaw, Poland), respectively. The cells were cultured in Dulbecco's modified Eagle's medium (DMEM, Institute of Immunology and Experimental Therapy (IITD), Poland) containing 10% fetal bovine serum (FBS, Gibco, USA) and 1% penicillin/streptomycin (Gibco, USA) at 37 ºC in 5% CO_2. For all the experiments, the A375 cells and HT29 cells were used at 80% confluence following 2–6 passages.

MTT assay for cytotoxicity of compounds

Cytotoxic effects of compounds against the A375 and HT29 cells were determined by MTT (3-(4,5-dimethylthiazol-2-yl)-2,5-diphenyltetrazolium bromide) (Sigma, St Louis, MO, USA) cell proliferation assay.[85] Briefly, the A375 and HT29 cells were plated in 96 well plates (1×10^4 cells/well) and were allowed to attach for 24 h. Then, the tested ligands (with or without Mg^{2+} and Ca^{2+}) were added to obtain the final concentration in the range of (0-1000 μM) and the cells were incubated for 48 h. After incubation, cell viability was assessed by incubating the cells with 0.5 mg mL^{-1} of MTT for another 4 h. Then, the supernatants were removed from the plates and the precipitated formazan was dissolved in 50 mL DMSO. Next, the plates were read under 570 nm using a Multiskan GO absorbance reader (Thermo Scientific, USA). All experiments were carried out in triplicate. The results were expressed as mean ± SD. The IC_{50} values (μM) were defined as the compound concentrations reducing absorbance to 50 % of control values.

Authors Contributions

JG conceived and designed studies and wrote the paper. ECh synthesized ligands, evaluated their structures and interpreted NMR spectra. JG (potentiometry, UV-vis, ITC, lipophilicity measurements), H.C-I (ESI-MS) and TJ (biological studies) performed the experiments. PK reviewed the paper. All authors read and approved the manuscript.

Conflicts of Interest

There are no conflicts to declare.

Acknowledgements

ITC and UV-vis measurements were performed (JG) at the Laboratory of Elemental Analysis and Structural Research and the cells were cultured (TJ) in the Screening Laboratory of Biological Activity Test and Collection of Biological Material, both laboratories located at the Faculty of Pharmacy and the Division of Laboratory Diagnostics, Wroclaw Medical University, supported by the ERDF Project within the Innovation Economy Operational Programme POIG.02.01.00-14-122/09. Project supported by Wrocław Centre of Biotechnology, programme The Leading National Research Centre (KNOW) for years 2014-2018 (ECh).

References

1 F. H. Ebetino, A. L. Hogan, S. Sun, M. K. Tsoumpra, X. Duan, J. T. Trif, A. A. Kwaasi, J. E. Dunford, B. L. Barnett, U. Oppermann, M. W. Lundy, A. Boyde, B. A. Kashemirov, C. E. Mckenna and R. G. G. Russell, *Bone*, 2011, **49**, 20–33.
2 R. G. G. Russell, *Bone*, 2011, **49**, 2–19.
3 L. E. Cole, T. Vargo-Gogola and R. K. Roeder, *Adv. Drug Deliv. Rev.*, 2016, **99**, 12–27.
4 M. Tauro, F. Loiodice, M. Ceruso, C. T. Supuran and P. Tortorella, *Bioorganic Med. Chem. Lett.*, 2014, **24**, 1941–1943.
5 E. Kotsikorou, Y. Song, J. M. W. Chan, S. Faelens, Z. Tovian, E. Broderick, N. Bakalara, R. Docampo and E. Oldfield, *J. Med. Chem.*, 2005, **48**, 6128–6139.
6 P. Kosikowska, M. Bochno, K. Macegoniuk, G. Forlani, P. Kafarski and Ł. Berlicki, *J. Enzyme Inhib. Med. Chem.*, 2016, **31**, 931–8.
7 J. Gałęzowska, *ChemMedChem*, 2018, **13**, 289–302.
8 S. G. Rotman, D. W. Grijpma, R. G. Richards, T. F. Moriarty, D. Eglin and O. Guillaume, *J. Control. Release*, 2018, **269**, 88–99.
9 H. Studnik, S. Liebsch, G. Forlani, D. Wieczorek, P. Kafarski and J. Lipok, *N. Biotechnol.*, 2015, **32**, 1–6.
10 K. Popov, H. Rönkkömäki and L. Lajunen, *Pure Appl. Chem.*, 2001, **73**, 1641–1677.
11 E. Matczak-Jon and V. Videnova-Adrabińska, *Coord. Chem. Rev.*, 2005, **249**, 2458–2488.
12 S. Bauhsina, P. Buglyo, E. Abi Aad, A. Aboukais and T. Kiss, 2004, **357**, 305–310.
13 S. E. Papapoulos, *Bone*, 2006, **38**, 613–616.
14 D. K. Wysowski and P. Greene, *Bone*, 2013, **57**, 423–428.
15 H. Hirabayashi and J. Fujisaki, *Clin. Pharmacokinet.*, 2003, **42**, 1319–1330.
16 A. I. Brenner, J. Koshy, J. Morey, C. Lin and J. Dipoce, *Semin. Nucl. Med.*, 2012, **42**, 11–26.
17 R. E. Coleman and E. V. McCloskey, *Bone*, 2011, **49**, 71–76.
18 J. Porta-Sales, C. Garzón-Rodríguez, S. Llorens-Torromé, C. Brunelli, A. Pigni and A. Caraceni, *Palliat. Med.*, 2017, **31**, 5–25.
19 V. Bousson, T. Leturcq, H.-K. Ea, O. Hauger, N. Mehsen-Cetre, B. Hamzé, C. Parlier-Cuau, J.-D. Laredo, T. Schaeverbeke and P. Orcel, *Eur. Radiol.*, 2018, **28**, 478–486.
20 S. L. Silverman, R. Landesberg, A. Greenspan, et al., P. White and B. Henderson, *Am. J. Med.*, 2009, **122**, S33–S45.
21 O. Filleul, E. Crompot and S. Saussez, *J. Cancer Res. Clin. Oncol.*, 2010, **136**, 1117–1124.
22 M. Pazianas, J. Compston and C. L.-H. Huang, *J. Bone Miner. Res.*, 2010, **25**, 2–10.
23 S. Khosla, J. P. Bilezikian, D. W. Dempster, E. M. Lewiecki, P. D. Miller, R. M. Neer, R. R. Recker, E. Shane, D. Shoback and J. T. Potts, *J. Clin. Endocrinol. Metab.*, 2012, **97**, 2272–2282.
24 M. Fazil, S. Baboota, J. K. Sahni, Ameeduzzafar and J. Ali, *Drug Deliv.*, 2014, **7544**, 1–9.
25 L. Forte, P. Torricelli, E. Boanini, M. Gazzano, M. Fini and A. Bigi, *Acta Biomater.*, 2017, **54**, 419–428.

DOI: 10.1039/C8NJ01158C

26 A. Bigi and E. Boanini, *J. Appl. Biomater. Funct. Mater.*, 2017, **15**, e313–e325.
27 M. Parent, H. Baradari, E. Champion, C. Damia and M. Viana-Trecant, *J. Control. Release*, 2017, **252**, 1–17.
28 I. J. Macha, S. Cazalbou, R. Shimmon, B. Ben-nissan and B. Milthorpe, 2017, 1723–1731.
29 K. Farbod, A. Curci, M. Diba, T. Zinkevich, A. P. Kentgens, M. Lafisco, N. Margiotta and S. C. G. Leeuwenburgh, *RSC Adv.*
30 L. De Luca, A. Chiminazzo, L. Sperni, G. Strukul and A. Scarso, *Chem. - A Eur. J.*, 2017, **23**, 3474–3478.
31 S. L. Silverman, N. B. Watts, P. D. Delmas, J. L. Lange and R. Lindsay, *Osteoporos. Int.*, 2007, **18**, 25–34.
32 S. Suri, J. Mönkkönen, M. Taskinen, J. Pesonen, M. A. Blank, R. J. Phipps and M. J. Rogers, *Bone*, 2001, **29**, 336–343.
33 S. Kasimir-Bauer, K. Reiter, B. Aktas, A.-K. Bittner, S. Weber, T. Keller, R. Kimmig and O. Hoffmann, *Sci. Rep.*, 2016, **6**, 26355.
34 J. Zekri, M. Marples, D. Taylor, K. Kandukurti, L. McParland and J. E. Brown, *J. Bone Oncol.*, 2017, **8**, 13–17.
35 P.407922 (A1 407922), date 2014-04-16, 2014.
36 W. Goldeman and A. Nasulewicz-Goldeman, *Bioorganic Med. Chem. Lett.*, 2014, **24**, 3475–3479.
37 E. Dabrowska, A. Burzyńska, A. Mucha, E. Matczak-Jon, W. Sawka-Dobrowolska, Ł. Berlicki and P. Kafarski, *J. Organomet. Chem.*, 2009, **694**, 3806–3813.
38 E. Chmielewska and P. Kafarski, *Molecules*, , DOI:10.3390/molecules21111474.
39 E. Bálint, Á. Tajti, A. Dzielak, G. Hägele and G. Keglevich, *Beilstein J. Org. Chem.*, 2016, **12**, 1493–1502.
40 E. Boanini, M. Gazzano and A. Bigi, *J. Phys. Chem. C*, 2012, **116**, 15812–15818.
41 F. Errassifi, S. Sarda, A. Barroug, A. Legrouri, H. Sfihi and C. Rey, *J. Colloid Interface Sci.*, 2014, **420**, 101–111.
42 V. Kubíček, J. Kotek, P. Hermann and I. Lukeš, *Eur. J. Inorg. Chem.*, 2007, 333–344.
43 J. R. Zeevaart, N. V. Jarvis, W. K. A. Louw, G. E. Jackson, I. Cukrowski and C. J. Mouton, *J. Inorg. Biochem.*, 1999, **73**, 265–272.
44 M. Szpak, A. Kamecka, B. Kurzak and W. Goldeman, *Polyhedron*, 2017, **123**, 385–395.
45 B. Kurzak, W. Goldeman, M. Szpak, E. Matczak-Jon and A. Kamecka, *Polyhedron*, 2015, **85**, 675–684.
46 E. Matczak-Jon, V. Videnova-Adrabińska, A. Burzyńska, P. Kafarski and T. Lis, *Chem. - A Eur. J.*, 2005, **11**, 2357–2372.
47 C. W. Childs, *Inorg. Chem.*, 1970, **9**, 2465–2469.
48 S. Bandyopadhyay, A. Das, G. N. Mukherjee, A. Cantoni, G. Bocelli, S. Chaudhuri and J. Ribas, *Inorganica Chim. Acta*, 2004, **357**, 3563–3573.
49 C. Bogdán, G. Péczely and F. Gaizer, *Polyhedron*, 2001, **20**, 1809–1813.
50 M. Dyba, Jezowska-Bojczuk, E. Kiss, T. Kiss, H. Kozlowski, Y. Leroux and D. El Manouni, *J. Chem. Soc. Dalt. Trans.*, 1996, 1119–1123.
51 J. R. Zeevaart, D. R. Jansen, M. Filomena Botelho, A. Abrunhosa, C. Gomes, L. Metello, Z. I. Kolar, G. C. Krijger, W. K. A. Louw and I. C. Dormehl, *J. Inorg. Biochem.*, 2004, **98**, 1521–1530.
52 J. Gałęzowska, R. Janicki, A. Mondry, R. Burgada, T. Bailly, M. Lecouvey and H. Kozłowski, *Dalton Trans.*, 2006, 4384–94.
53 B. Kurzak, A. Kamecka, K. Kurzak, J. Jezierska and P. Kafarski, *Polyhedron*, 1998, **17**, 4403–4413.
54 E. Matczak-Jon, B. Kurzak, P. Kafarski and A. Woźna, *J. Inorg. Biochem.*, 2006, **100**, 1155–1166.
55 E. Matczak-Jon, T. Kowalik-Jankowska, K. Slepokura, P. Kafarski and A. Rajewska, *Dalton Trans.*, 2010, **39**, 1207–21.
56 E. Matczak-Jon, B. Kurzak and W. Sawka-Dobrowolska, *Polyhedron*, 2012, **31**, 176–187.
57 C. Foti, O. Giuffrè and S. Sammartano, *J. Chem. Thermodyn.*, 2013, **66**, 151–160.
58 H. A. Habib, B. Gil-Hernández, K. Abu-Shandi, J. Sanchiz and C. Janiak, *Polyhedron*, 2010, **29**, 2537–2545.
59 E. Gumienna-Kontecka, J. Jezierska, M. Lecouvey, Y. Leroux and H. Kozlowski, *J. Inorg. Biochem.*, 2002, **89**, 13–17.
60 T. Kowalik-Jankowska, M. Pietruszka, J. Jezierska, E. Matczak-Jon and P. Kafarski, *Polyhedron*, 2011, **30**, 1274–1280.
61 M. Sikorska, M. Gazda and J. Chojnacki, *Acta Crystallogr. Sect. E Struct. Reports Online*, 2012, **68**, 887–897.
62 V. Deluchat, J. C. Bollinger, B. Serpaud and C. Caullet, *Talanta*, 1997, **44**, 897–907.
63 B. Demoro, S. Rostán, M. Moncada, Z.-H. Li, R. Docampo, C. Olea Azar, J. D. Maya, J. Torres, D. Gambino and L. Otero, *J. Biol. Inorg. Chem.*, 2018, **23**, 303–312.
64 E. Matczak-jon, B. Kurzak, A. Kamecka, W. Sawka-Dobrowolska and P. Kafarski, 1999, 3627–3637.
65 N. E. Grossoehme, A. M. Spuches and D. E. Wilcox, *J. Biol. Inorg. Chem.*, 2010, **15**, 1183–1191.
66 J. Gałęzowska, H. Czapor-Irzabek, R. Janicki, E. Chmielewska and T. Janek, *New J. Chem.*, 2017, **41**, 10731–10741.
67 M. A. Mostefa Side Larbi, C. Sauzet, P. Piccerelle, P. Cau, N. Levy, P. Gallice and D. Berge-Lefranc, *J. Chem. Thermodyn.*, 2016, **97**, 290–296.
68 R. L. Carroll and R. R. Irani, *J. Inorg. Nucl. Chem*, 1968, **30**, 2971–2976.
69 Y. V. Griko, *Biophys. Chem.*, 1999, **79**, 117–127.
70 G. Schwarzenbach and G. Anderegg, *Helv. Chim. Acta*, 1957, **40**, 1773–1792.
71 OECD, in *OECD Guidelines for the Testing of Chemicals; Section 1: Physical–Chemical Properties; OECD Publishing, Paris*, 1995, vol. 107, pp. 1–4.
72 G. Ananchenko, J. Novakovic and A. Tikhomirova, *Profiles of Drug Substances, Excipients and Related Methodology*, Academic Press, Elsevier, San Diego, 2013.
73 H. Sanderson and M. Thomsen, *Toxicol. Lett.*, 2009, **187**, 84–93.
74 T. Hiraga, T. Nakajima and H. Ozawa, *Bone*, 1995, **16**, 349–56.
75 S. G. Senaratne, G. Pirianov, J. L. Mansi, T. R. Arnett and K. W. Colston, *Br. J. Cancer*, 2000, **82**, 1459–1468.
76 X. Huang, R. Huang, Z. Liao, Y. Pan, S. Gou and H. Wang, *Eur. J. Med. Chem.*, 2016, **108**, 381–391.
77 WO2015/159153, A1, 2015-10-22, 2015.
78 Y. Takeuchi, M.; Sakamoto, S.; Yoshida, M.; Abe, T.; Isomura, *Chem Pharm Bull.*, 1993, **41**, 688–693.
79 H. M. Irving, M. G. Miles and L. D. Pettit, *Anal. Chim. Acta*, 1967, **38**, 475–488.
80 G. Gran, *Acta Chem. Scand.*, 1950, **4**, 559–577.
81 P. Gans, A. Sabatini and A. Vacca, *Talanta*, 1996, **43**, 1739–1753.

View Article Online
DOI: 10.1039/C8NJ01158C

82 P. Gans, *Data Fitting in the Chemical Sciences: By the Method of Least Squares*, WILEY-VCH Verlag, 1992.
83 L. Alderighi, P. Gans, A. Ienco, D. Peters, A. Sabatini and A. Vacca, *Coord. Chem. Rev.*, 1999, **184**, 311–318.
84 www.hyperquad.co.uk.
85 T. Mosmann, *J. Immunol. Methods*, 1983, **65**, 55–63.

View Article Online
DOI: 10.1039/C8NJ01158C

Graphical Abstract

Figure

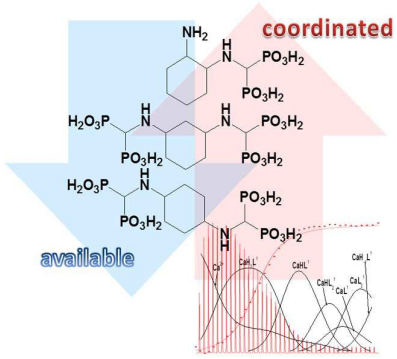

Synopsis

Complex formation equilibria of calcium, magnesium, copper and nickel with amino-bisposphonic ligands is described, together with a speciation study along with calorimetric outcome and cytotocixity characteristics..